

Thermal and flow characteristics of microchannel heat sink with rectangular grooves using nanofluids

Xiaoxin Zeng¹, Quanyi Liu¹, Hao Yu¹, Ning Mao^{1,2*}

¹ Department of Gas Engineering, College of Pipeline and Civil Engineering, China University of Petroleum (East China), Qingdao, China

² Institute of Industrial Science, The University of Tokyo, Tokyo, Japan

ABSTRACT

Microchannel heat sink is one of the most promising cooling solutions for electronics with high heat flux. In order to further enhance the heat transfer performance of microchannel heat sink, a novel microchannel with rectangular grooves on the wall is designed, and the heat transfer and flow characteristics of Al₂O₃/water nanofluid in microchannels are numerically studied. The mixture model is used involving the slip velocity between nanoparticles and base fluid. By comparing with the conventional smooth channel, it's found that grooves are helpful to destroy and redevelop the thermal boundary layer. The disturbance by grooves also leads to much higher pressure drop through the channel than smooth one. This work will be helpful for the design of high-performance microchannel heat sink.

Keywords: microchannel, rectangular groove, nanofluid, heat transfer, flow

NONMENCLATURE

Symbols	
a	Acceleration, m/s^2
C_p	Specific heat capacity, $J/(kg \cdot K)$
d	Diameter, m
D	Hydraulic diameter, m
E	Depth of rectangular groove, m
g	Gravitational acceleration, m/s^2
H	Height of microchannel, m
j	Heat transfer factor
K_{nf}	Knudsen number
L	Length of heat sink, mm
Nu	Nusselt number
p	Pressure, Pa
Pr	Prandtl number
q	Heat flux, W/cm^2
Re	Reynolds number
T	Temperature, K
u	Inlet velocity, m/s
V	Velocity, m/s
W	Width of microchannel, m
ρ	Mass density of fluid, kg/m^3

μ	Kinematic viscosity, $Pa \cdot s$
-------	-----------------------------------

1. INTRODUCTION

The miniaturization of electronic devices continuously compresses the space for heat dissipation. Consequently, the heat flux of electronic chip with high integration has reached the magnitude of MW/m^2 , which made the existing cooling methods no longer meet the heat dissipation requirement. Microchannel heat sink is one of the most compact and powerful cooling apparatus to remove high heat flux[1]. Tuckerman and Pease[2] first designed and tested a rectangular microchannel heat sink to cool down the integrated circuits. The allowable heat flux was reported as high as $1700W/cm^2$ with only $70^\circ C$ temperature rise of the micro-chip.

To improve the thermal performance of microchannel heat sink, structural optimization is commonly considered. Lin et al. [3] found that the curved walls of corrugated microchannel radiators promote the mixing of coolants and enhance the convection heat transfer between the coolant and the wall. Cheng et al.[4] designed a microchannel with uniformly offset fins, which facilitates the diffusion of the thermal boundary layer and enhances heat transfer. Han et al. [5] designed a uniform internal vertical bifurcation microchannel to improve the thermal performance of the microchannel.

Due to the limiting cooling ability of conventional coolants such as water and ethylene glycol, it may not meet the heat dissipation demand under high heat flux condition. Choi and Eastman[6] firstly introduced nanofluid to this issue, which is composed of nano-sized metal particles suspended in water. Since the nano additions largely improve the thermal conductivity of the fluid, the heat transfer efficiency was greatly enhanced[7]. Thansekhar et al.[8] experimentally found that a higher volume concentration of nanofluid contributes better heat transfer performance while additional pressure drop caused by nanofluid is not very high. Li et al.[9] found that Al₂O₃/water nanofluid has significant effect on thermal performance, however it has the disadvantage of increasing energy consumption. The mostly used single-phase model assumes that the

fluid phase and particles are in thermal equilibrium, and there is no slip velocity between them[10]. Then the fluid properties are only to be calculated before simulation. However, the simple assumptions may cause deviation by neglecting mixing effects between two phases. Yet, the advanced two-phase mixture models allow interpenetrating phases in a control volume, which means that each phase has its own velocity and volume fraction. Akbari et al.[11] comparatively studied single-phase model and three different two-phase models (VOF, mixture and Eulerian model). The results show that the convective heat transfer coefficient of two-phase models agrees better with the experimental data. Similar results are found out by Fard et al.[12] who studied the convective heat transfer of nanofluids in circular tube.

In order to further enhance the heat transfer performance of nanofluid in microchannel, rectangular grooves were constructed in the microchannel as a novel structural design in this study. The Al_2O_3 /water was selected as coolant, and was simulated using the mixture model. The heat transfer enhancement mechanism of

nanofluid in microchannels was explored. The flow and heat transfer characteristics of different volume fractions of nanofluid in complex structural microchannels were also systematically investigated.

2. NUMERICAL METHOD

2.1 Physical model

The microchannel in this study is according to a previous study[13], as shown in Fig. 1, and the experimental data are used to verify the proposed simulation method. The microchannel heat sink consists of 21 parallel channels, the schematic diagram of microchannel heat sink is shown in Fig. 1. One channel is selected as computing zone, as shown in Fig. 1, which includes solid domain (channel wall) and fluid domain (channel). Fig. 1 shows the schematic diagram of the computing zone. The material of heat sink is copper and the cover plate is of polycarbonate plastic. A constant heat flux q_w is applied at the bottom of microchannel, and the other walls are assumed to be adiabatic.

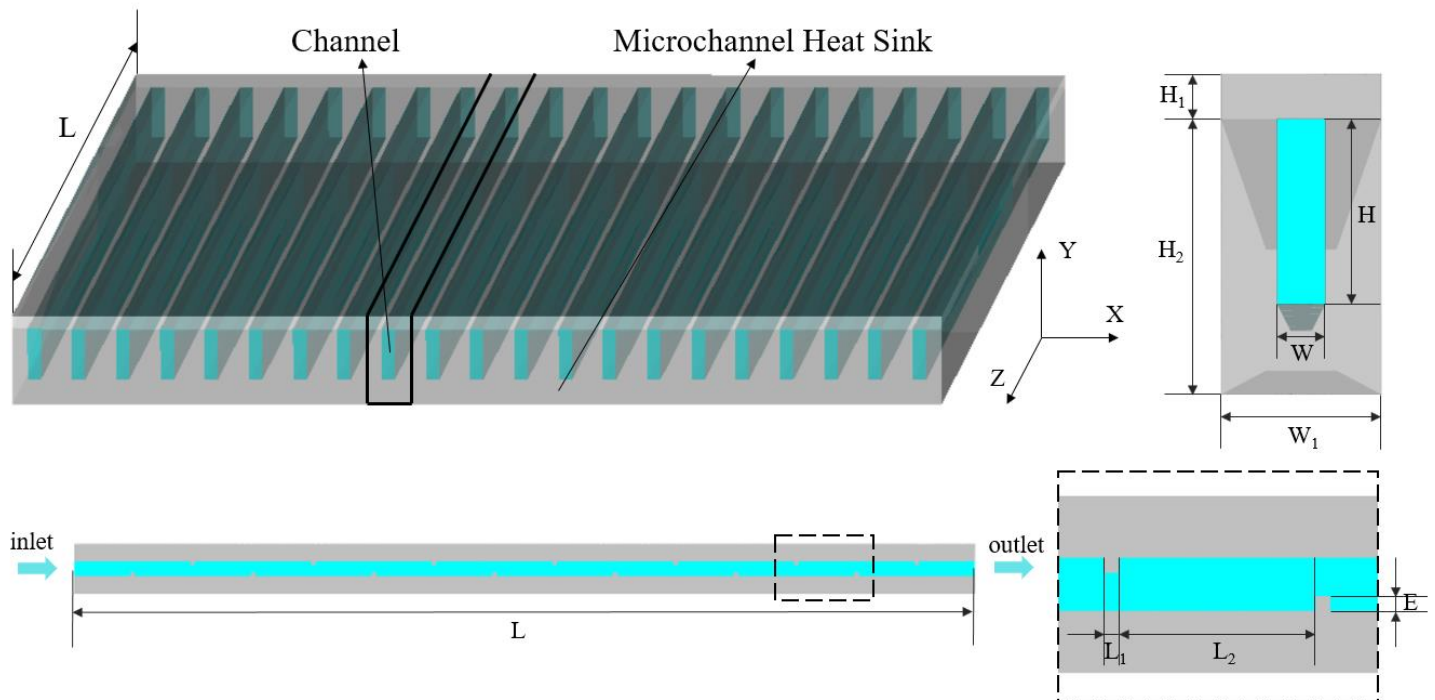


Fig. 1 Schematic diagram of microchannel heat sink.

Table 1 Parameters for different configuration of the microchannel.

Case	Feature	L (mm)	L ₁ (μ m)	L ₂ (μ m)	E (μ m)	H (μ m)	H ₁ (μ m)	H ₂ (μ m)	W (μ m)	W ₁ (μ m)
0	smooth	44.8	\	\	\	821	200	1221	215	715
1	smooth	12.84	\	\	\	821	200	1221	215	715
2	grooved	12.84	60	800	60	821	200	1221	215	715

In this study, Case 0 and Case 1 is smooth rectangular microchannel and Case 2 is microchannel with rectangular grooves. Case 0 is used for model validation comparing with experiment, its length (L) is 44.8mm. Case 1 and Case 2 are used for further comparative study, their length (L) is 12.84mm. The width of the calculation field (W_1) is $715\mu m$. The total thickness of copper-based microchannel (H_2) is $1221\mu m$. The thickness of polycarbonate plastic cover (H_1) is $200\mu m$. The width (W) and height (H) of the microchannel are $215\mu m$ and $821\mu m$ respectively. The specific structure of Case 2 (microchannel with rectangular grooves) is shown in Fig. 1(b). The width of rectangular groove (L_1) is $60\mu m$, the depth of rectangular groove (E) is $60\mu m$ and the distance between rectangular grooves (L_2) is $800\mu m$. The detailed geometric parameters are listed in

1.

2.2 Mathematical model

The following assumptions are considered:

- 1) The flow and heat transfer process are steady state;
- 2) The fluid is incompressible, the nanoparticles are uniformly distributed in the base fluid;
- 3) The viscous dissipation of nanofluid is considered.

The mixture model assumes that there is a well coupling between the primary phase and the secondary phase, with particles closely following the flow. Supposing that there is an interpenetration between the primary phase and the secondary phase, it means that both phases have their own velocity vector field, volume fractions of the primary phase and the secondary phase exist in each control volume. The mixture model doesn't use the governing equations of any phase separately, the continuity equation, the momentum equation and the energy equation of the mixture are used.

Then the equations describing the flow and heat transfer of nanofluids in microchannels are presented as follows[14]:

(1) Fluid domain

Continuity equation:

$$\nabla(\rho_{nf} V_m) = 0 \quad (1)$$

Momentum equation:

$$\nabla(\rho_{nf} V_m V_m) = -\nabla P + \nabla(\mu_{nf} \nabla V_m) + \rho_{nf} g + \nabla\left(\sum_{k=1}^n \phi_k \rho_k V_{dr,k} V_{dr,k}\right) \quad (2)$$

Energy equation:

$$\nabla\left(\sum_{k=1}^n \rho_k C_{pk} \phi_k V_k T\right) = \nabla(K_{nf} \nabla T) + \tau \quad (3)$$

Volume fraction equation:

$$\nabla(\phi_p \rho_p V_m) = -\nabla(\phi_p \rho_p V_{dr,p}) \quad (4)$$

ρ_{nf} is the mixture density:

$$\rho_{nf} = (1 - \phi) \rho_{bf} + \phi \rho_p \quad (5)$$

V_m is mass average velocity:

$$V_m = \frac{\sum_{k=1}^n \phi_k \rho_k V_k}{\rho_{nf}} \quad (6)$$

$V_{dr,k}$ is the drift velocity of nanoparticles:

$$V_{dr,k} = V_k - V_m \quad (7)$$

The slip velocity (relative velocity) is defined as the velocity of nanoparticle relative to the velocity of the base fluid:

$$V_{pf} = V_p - V_{bf} \quad (8)$$

Drift velocity is related to slip velocity according to the following relation:

$$V_{dr,p} = V_{bf} - \sum_{i=1}^n \frac{\phi_i \rho_i}{\rho_{nf}} V_{f,i,k} \quad (9)$$

$$V_{pf} = \frac{\rho_p d_p^2}{18 \mu_{bf} f_{drag}} \frac{(\rho_p - \rho_{nf})}{\rho_p} a \quad (10)$$

In the above equation, f_{drag} is the drag function and can be defined as follows:

$$f_{drag} = f(x) = \begin{cases} 1 + 0.15 \text{Re}_p^{0.687}, & \text{Re}_p \leq 1000 \\ 0.0183 \text{Re}_p, & \text{Re}_p \geq 1000 \end{cases} \quad (11)$$

(2) Solid domain

Energy equation in the solid domain:

$$k_s \left(\frac{\partial^2 T}{\partial x^2} + \frac{\partial^2 T}{\partial y^2} + \frac{\partial^2 T}{\partial z^2} \right) = 0 \quad (12)$$

k_s is the thermal conductivity of the solid domain.

Table 2 Thermophysical properties of water and nanoparticle.

Property	Water	Alumina
Density (kg/m^3)	998.2	3970
Specific heat ($J/kg \cdot K$)	4182	765
Thermal conductivity ($W/m \cdot K$)	$-0.93314 + 0.00853 \cdot T - 0.000011259 \cdot T^2$	25
Viscosity ($kg/m \cdot s$)	$0.01723 - 9.25951e-5 \cdot T + 1.2681e-7 \cdot T^2$	

2.3 Thermal properties

Al₂O₃/water nanofluid is considered in this work. The diameter of Al₂O₃ particle is 36 nm, the volume fraction of nanoparticle varies from 0.5% to 1%. The thermophysical properties of water and the nanoparticle are shown in Table 2[15].

The density and specific heat of nanofluids are mostly calculated using mixing theory[16]. For the density of nanofluids:

$$\rho_{nf} = (1-\varphi)\rho_{bf} + \varphi\rho_p \quad (13)$$

where ρ_{bf} and ρ_p represent the density of the base fluid and nanoparticles, respectively. φ represents the volume fraction of nanoparticles in nanofluids.

For the specific heat of nanofluids:

$$C_{pmf} = \frac{(1-\varphi)\rho_{bf}C_{pbf} + \varphi\rho_pC_{pp}}{(1-\varphi)\rho_{bf} + \varphi\rho_p} \quad (14)$$

where C_{pbf} and C_{pp} represent the specific heat of base fluid and the nanoparticle.

According to the Hamilton-Crosser model[17], thermal conductivity is a function of particle shape and volume fraction, while the enhanced heat conduction effect caused by the random movement of particles in the base fluid isn't included. Considering that particles in this study are spherical particles, it is defined as follows:

$$k_{nf} = \frac{k_p + 2k_{bf} - 2\varphi(k_{bf} - k_p)}{k_p + 2k_{bf} + \varphi(k_{bf} - k_p)} k_{bf} \quad (15)$$

where k_{bf} and k_p represent the thermal conductivity of base fluid and the nanoparticle, respectively.

Effective viscosity of the Al₂O₃/water nanofluid is defined by Einstein model[18]:

$$\mu_{nf} = (1 + 2.5\varphi)\mu_{bf} \quad (16)$$

where μ_{bf} represents the viscosity of base fluid.

2.4 Boundary conditions

The Reynolds number in this study is ranged from 150 to 750, which is a common regime according to literature[19]. Constant heat flux boundary condition is adopted at the bottom of the microchannel heat sink. The solid-fluid interface is coupling boundary. The rest walls are assumed to be adiabatic, as seen in Fig. 1(b). The detailed boundary conditions are as follows:

- At the inlet: $u=u_{in}$, $v=0$, $w=0$, $T_{in}=303.16$ K;
- At the outlet: $p=p_{out}=1$ atm;

3. RESULTS AND DISCUSSION

3.1 Model validation

- At the fluid-solid interfaces: $u=0$, $v=0$, $w=0$, $T_s=T_f$, $k_s \frac{\partial T_s}{\partial n} = k_{nf} \frac{\partial T_f}{\partial n}$;
- At the bottom surface: $q_w = -k_s \frac{\partial T_s}{\partial z} = 20$ W/cm² (for model reliability verification), $q_w = -k_s \frac{\partial T_s}{\partial z} = 80$ W/cm² (for this study);
- At other wall surfaces: $\frac{\partial T_s}{\partial n} = 0$;

where T_f is the temperature of the nanofluid near the wall. T_s is the wall temperature. n represents the normal direction of the interface.

2.5 Numerical method

The computing domain is divided into three independent blocks, including nanofluid, solid wall and cover plate. Hexahedral mesh is generated Using ANSYS ICEM 2021. For Case 0, four different numbers of grids (580 k, 1060 k, 1960 k and 3780 k) are used in the grid independence test. The temperature variation curves on the center line of the bottom surface of four different grid heat sinks are shown in Fig. 2. The difference of the results calculated by the latter three grids is less than 1%, so 1060 k grid numbers are selected for calculation.

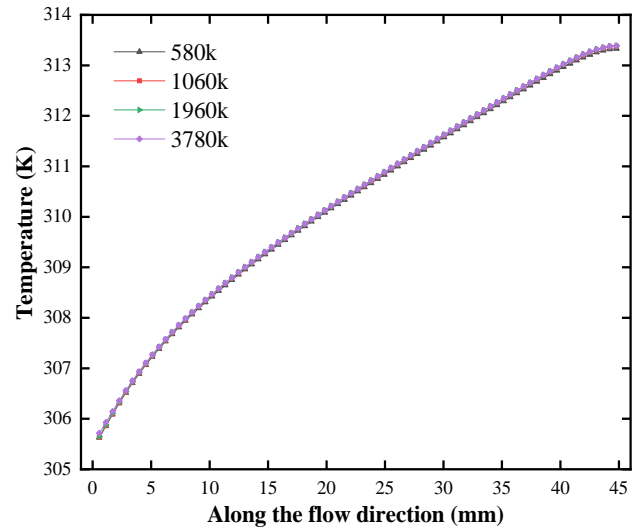


Fig. 2 Mesh independence verification.

The computation is carried out using the commercial CFD software FLUENT 2021. The simulation uses the Pressure-Based solver. The SIMPLE algorithm is used to couple the pressure and velocity. The QUICK algorithm is used to solve the discrete volume fraction. The momentum equation and energy equation use the Second Order Upwind scheme for solving. Converged results are obtained after the residuals satisfy energy residual and momentum residual less than 10^{-6} .

The proposed simulation method is verified by comparing with the experimental data in literature[13]. The wall temperature is measured along the axis of the

microchannel heat sink, and the specific measurement points are shown in the literature. Case0 is studied.

The heat transfer of Al_2O_3 /water nanofluids with volume fraction of 1% in rectangular microchannel is simulated and the results are shown in Fig. 3. The results show that the calculated results of mixture model agree well with experimental data. In particular, the simulation results based on mixture model have higher accuracy when the mass flow rate increases.

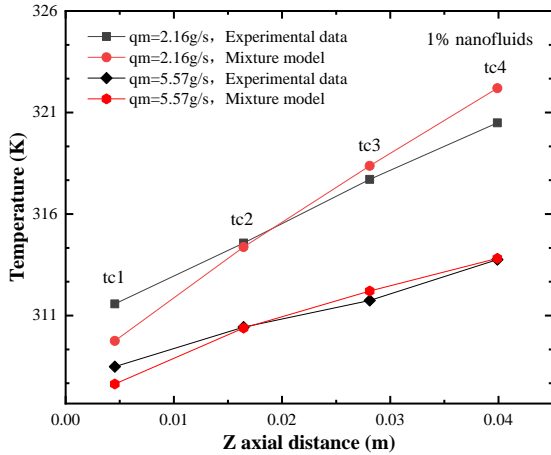


Fig. 3 Wall temperature along the axial direction at different flow rates.

Fig. 4 shows the pressure drop predicted by mixture model for the volume fraction of 2%. Comparing the experimental and numerical results, it can be found that the maximum error is only 2.03%. Therefore, the flow characteristics simulated based on mixture model also agree very well with experiments.

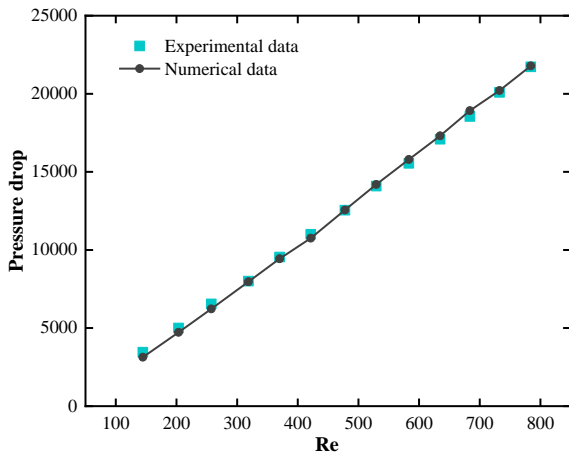


Fig. 4 Comparison of pressure drop between simulation and experiment

3.2 Heat transfer characteristics analysis

The maximum temperature (T_{max}) at the bottom surface of the microchannel heat sink is analyzed in this paper, which is the important indicator to evaluate the cooling performance of the heat sink.

As shown in Fig. 5, the maximum temperature (T_{max}) of Case 2 is significantly lower than that of Case 1. This is mainly due to the disturbance caused by the rectangular groove and the redevelopment of the thermal boundary layer. These effects become more significant with the increase of inlet velocity. The maximum temperature (T_{max}) of both microchannels decreases with increasing inlet velocity and volume fraction. The difference between the maximum temperature (T_{max}) between Case 1 and Case 2 increases with the increase of the inlet velocity. The inlet velocity has a greater impact on Case 2. Rectangular grooves in Case 2 can cause more severe disturbances at higher velocities. The difference of maximum temperature (T_{max}) between different volume fractions in Case 2 is slighter compared those with Case 1. The volume fractions of nanofluid has a greater impact on Case 1.

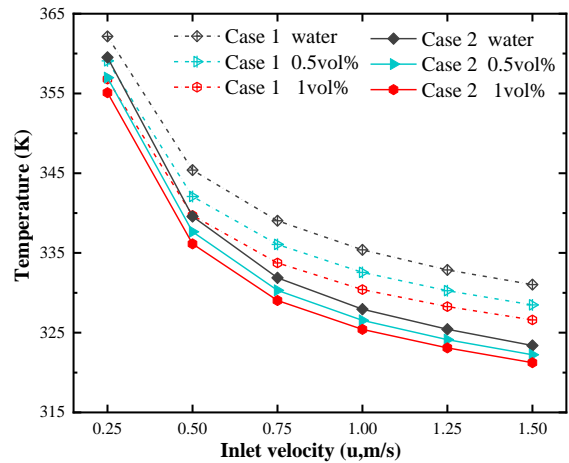


Fig. 5 T_{max} variation at different inlet velocities.

To better understand the influence of volume fractions of nanofluids and microchannel structure on heat transfer, Fig. 6 shows temperature contours. In the fluid domain, two planes are taken as shown in Fig. 6. Plane 1 is at $Z=0.0095$ m and the Plane 2 is at $Y=0.00081$ m. The temperature contours in Fig. 6 are captured over Plane 1 of Case 2 at the inlet velocity 0.25 m/s with different volume fractions. The results show that the temperature gradient near the rectangular grooves changes significantly with increasing volume fraction of nanofluids. The fluid temperature decreases near the wall and increases at the center with increasing volume fraction of nanofluids. The use of nanofluids improves the uniformity of temperature distribution in microchannels. With the increase of fluid thermal conductivity, the axial thermal conductivity effect is more significant and improve the heat transfer along axial, which helps carry more heat away. The temperature distribution contours in Fig. 6 are on the Plane 2 of different Case at the inlet velocity 1.25 m/s with volume fraction 0.5%. Compared with Case 1, the

fluid temperature near the wall of Case 2 decreases significantly and at the center increases slightly. Rectangular grooves increase the fluid disturbance and uniformity of temperature distribution in the microchannel. The asymmetric temperature distribution

is due to the arrangement of rectangular grooves. Both nanofluids and rectangular groove structures can reduce the local temperature of the microchannel and improve heat transfer performance.

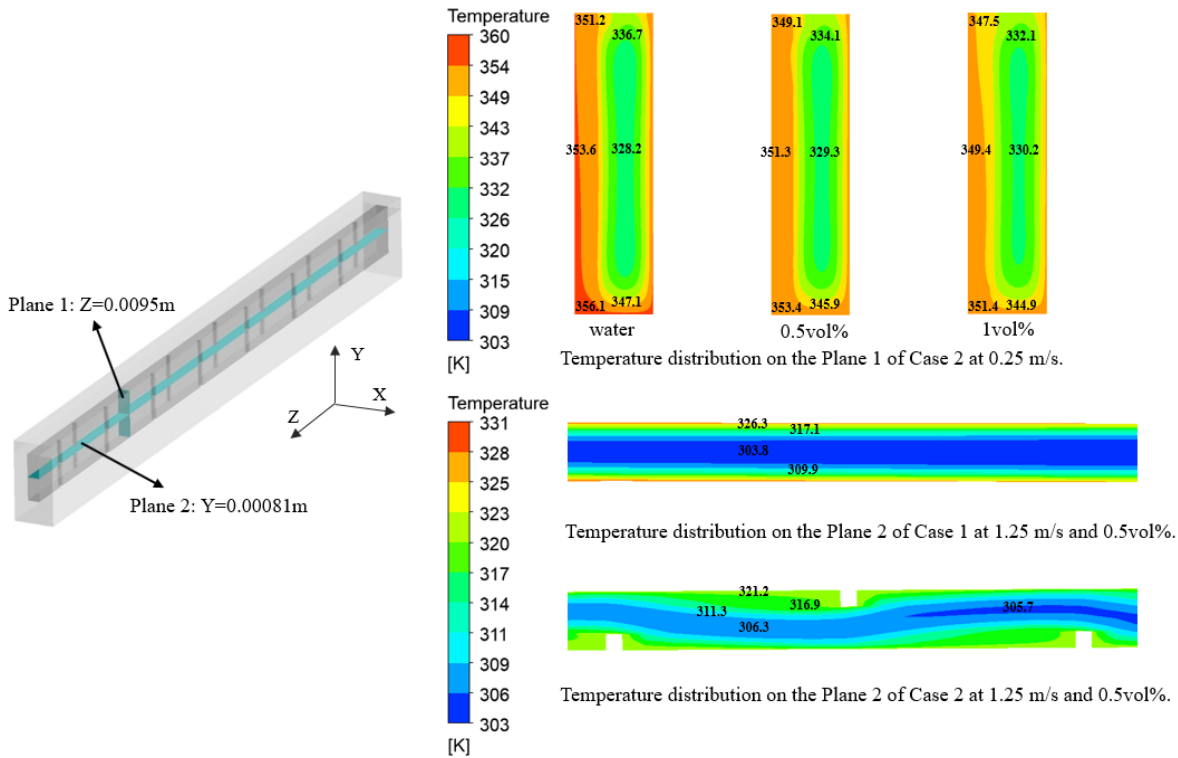


Fig. 6 The temperature distribution of Case 1 and Case2.

3.3 Flow characteristics analysis

In order to study the influence of nanofluid on the flow characteristics in microchannel, we analyzed the pressure drop of nanofluid in microchannel. In this study, laminar flow regime is only considered because the Reynolds number is ranged from 150 to 750, corresponding to inlet velocity from 0.25 m/s to 1.5 m/s.

Fig. 7 shows that the addition of nanoparticles increases the pressure drop, which is more pronounced with the increase of volume fraction of nanofluids. This is because the viscosity of nanofluids increases with higher volume fraction, resulting in higher flow resistance. Compared with Case 1, the turbulence caused by rectangular grooves of Case 2 has a significant effect on pressure drop, which is more obvious with the increase of inlet velocity. The pressure drop of Case 2 is 1.64-2.49 times that of Case 1. The rectangular grooves increase the turbulence and return flow in the microchannel, which are important factors affecting the pressure drop. It can also be found that the effect of volume fraction on pressure drop is not significant compared with inlet velocity. Compared with water, the

use of nanofluids does not significantly increase the pressure drop of microchannels, it is feasible to use nanofluids in microchannels considering this aspect.

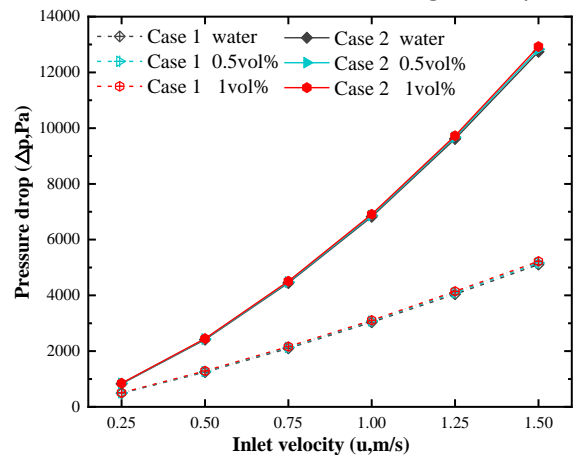


Fig. 7 Pressure drop at different inlet velocities.

The flow characteristics of fluids are actually closely related to the heat transfer characteristics. In order to further understand the flow and heat transfer characteristics of nanofluids in different microchannels, the velocity and temperature fields were further analyzed. As shown in Fig. 8, the rectangular grooves in

Case 2 have a significant effect on the velocity and temperature distribution in the flow field compared with Case 1. Disturbance occurs when the fluid in Case 2 passes through rectangular grooves in the direction of flow, forming swirls near the wall boundary layer, as shown in Fig. 8. It enhances the synergy between the velocity field and the temperature gradient field,

because the maximum temperature gradient is located at the wall boundary layer. The existence of rectangular groove will destroy the original thermal boundary layer and redevelop a new one. Therefore, Case 2 has better heat transfer characteristics than Case 1. Meanwhile, the formation of swirl further leads to the increase of pressure drop in microchannel.

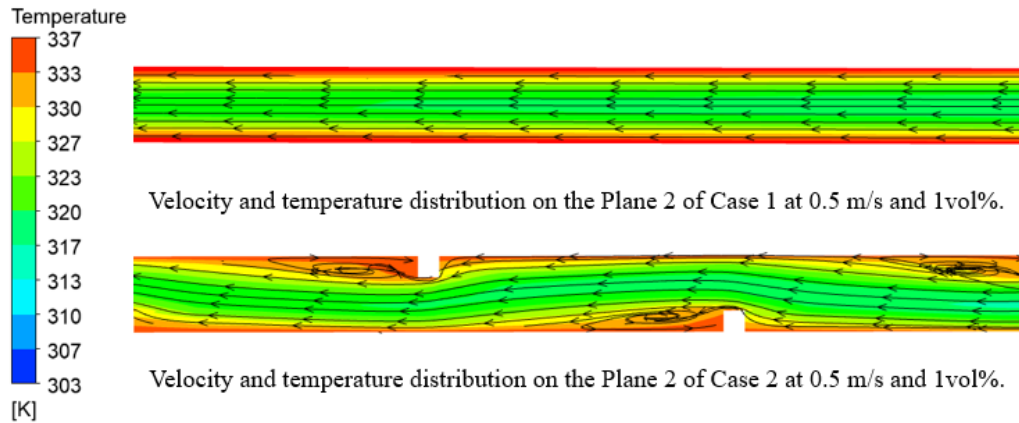


Fig. 8 Velocity and temperature distribution.

4. CONCLUSIONS

In this paper, the thermal and flow characteristics of Al_2O_3 /water nanofluid in microchannels with and without rectangular grooves are studied by using the mixture model. The following conclusions are obtained:

(1) With the increase of nanofluid inlet velocity and volume fraction, the heat transfer performance increases. The main reasons for the enhanced heat transfer of nanofluids in microchannels are the increase of the axial thermal conductivity of nanofluid with high thermal conductivity and thermal boundary layer thickness.

(2) The heat transfer performance of microchannel with rectangular grooves is better than that of smooth microchannel, but at a cost of greater pressure drop.

(3) There are three reasons why nanofluid in microchannels with rectangular grooves enhances heat transfer: the increase of the axial thermal conductivity in microchannel caused by nanofluid with high thermal conductivity, the destroyed and redeveloped thermal boundary layers by rectangular grooves, and disturbance effect brought by rectangular grooves.

(4) When the pump power consumption is not considered, the microchannel with rectangular groove is recommended for its better thermal performance. The use of nanofluids can further improve the heat transfer characteristics for microchannels.

The proposed grooved microchannel heat sink using Al_2O_3 /water nanofluid exhibits evidently better thermal performance than conventional smooth one using pure

water, which helps guiding for the design of high-performance microchannel heat sink.

ACKNOWLEDGEMENT

The study was supported by Shandong Provincial Natural Science Foundation, China (No.: ZR2020ME170), National Natural Science Foundation of China (No. 52276092) and Grant-in-Aid for JSPS Fellows (21F20056).

REFERENCE

- [1] Kandlikar SG. High flux heat removal with microchannels - A roadmap of challenges and opportunities. *Heat Transf Eng* 2005;26:5–14. <https://doi.org/10.1080/01457630591003655>.
- [2] Tuckerman, D.B., & Pease, R.F. High-Performance Heat Sinking for VLSI. *IEEE Electron Device Letters* 1981;2:126-9. <https://doi.org/10.1177/0164027595174002>.
- [3] Lin L, Zhao J, Lu G, Wang XD, Yan WM. Heat transfer enhancement in microchannel heat sink by wavy channel with changing wavelength/amplitude. *Int J Therm Sci* 2017;118:423–34. <https://doi.org/10.1016/j.ijthermalsci.2017.05.013>.
- [4] Hong F, Cheng P. Three dimensional numerical analyses and optimization of offset strip-fin microchannel heat sinks. *Int Commun Heat Mass Transf* 2009;36:651–6. <https://doi.org/10.1016/j.icheatmasstransfer.2009.02.015>.
- [5] Shen H, Wang CC, Xie G. A parametric study on thermal performance of microchannel heat sinks with

- internally vertical bifurcations in laminar liquid flow. *Int J Heat Mass Transf* 2018;117:487–97. <https://doi.org/10.1016/j.ijheatmasstransfer.2017.10.025>.
- [6] Choi SUS. Enhancing thermal conductivity of fluids with nanoparticles. *Am Soc Mech Eng Fluids Eng Div FED* 1995;231:99–105.
- [7] Alawi OA, Sidik NAC, Xian HW, Kean TH, Kazi SN. Thermal conductivity and viscosity models of metallic oxides nanofluids. *Int J Heat Mass Transf* 2018;116:1314–25. <https://doi.org/10.1016/j.ijheatmasstransfer.2017.09.133>.
- [8] Thansekhar MR, Anbumeenakshi C. Experimental Investigation of Thermal Performance of Microchannel Heat Sink with Nanofluids Al₂O₃/Water and SiO₂/Water. *Exp Tech* 2017;41:399–406. <https://doi.org/10.1007/s40799-017-0189-y>.
- [9] Li C, Huang J, Shang Y, Huang H. Study on the flow and heat dissipation of water-based alumina nanofluids in microchannels. *Case Stud Therm Eng* 2020;22:100746. <https://doi.org/10.1016/j.csite.2020.100746>.
- [10] Heris SZ, Esfahany MN, Etemad G. Numerical investigation of nanofluid laminar convective heat transfer through a circular tube. *Numer Heat Transf Part A Appl* 2007;52:1043–58. <https://doi.org/10.1080/10407780701364411>.
- [11] Akbari M, Galanis N, Behzadmehr A. Comparative analysis of single and two-phase models for CFD studies of nanofluid heat transfer. *Int J Therm Sci* 2011;50:1343–54. <https://doi.org/10.1016/j.ijthermalsci.2011.03.008>.
- [12] Haghshenas Fard M, Esfahany MN, Talaie MR. Numerical study of convective heat transfer of nanofluids in a circular tube two-phase model versus single-phase model. *Int Commun Heat Mass Transf* 2010;37:91–7. <https://doi.org/10.1016/j.icheatmasstransfer.2009.08.003>.
- [13] Lee J, Mudawar I. Assessment of the effectiveness of nanofluids for single-phase and two-phase heat transfer in micro-channels. *Int J Heat Mass Transf* 2007;50:452–63. <https://doi.org/10.1016/j.ijheatmasstransfer.2006.08.001>.
- [14] Mokhtari Moghari R, Akbarinia A, Shariat M, Talebi F, Laur R. Two phase mixed convection Al₂O₃-water nanofluid flow in an annulus. *Int J Multiph Flow* 2011;37:585–95. <https://doi.org/10.1016/j.ijmultiphaseflow.2011.03.008>.
- [15] Shi X, Li S, Wei Y, Gao J. Numerical investigation of laminar convective heat transfer and pressure drop of water-based Al₂O₃ nanofluids in a microchannel. *Int Commun Heat Mass Transf* 2018;90:111–20. <https://doi.org/10.1016/j.icheatmasstransfer.2017.11.007>.
- [16] Zhao JJ, Duan YY, Wang XD, Wang BX. Effect of nanofluids on thin film evaporation in microchannels. *J Nanoparticle Res* 2011;13:5033–47. <https://doi.org/10.1007/s11051-011-0484-y>.
- [17] Jiang F, Sousa ACM. Effective thermal conductivity of heterogeneous multi-component materials: An SPH implementation. *Heat Mass Transf Und Stoffuebertragung* 2007;43:479–91. <https://doi.org/10.1007/s00231-006-0131-9>.
- [18] Lisy V, Tothova J. On the (hydrodynamic) memory in the theory of Brownian motion 2004:1–12.
- [19] Li P, Guo D, Huang X. Heat transfer enhancement in microchannel heat sinks with dual split-cylinder and its intelligent algorithm based fast optimization. *Appl Therm Eng* 2020;171:115060. <https://doi.org/10.1016/j.applthermaleng.2020.115060>.